2009 American Control Conference
Hyatt Regency Riverfront, St. Louis, MO, USA
June 10-12, 2009

Validation of a Small Signal Probing Concept for Prognosis on a Nonlinear Model for Longitudinal Motion of a Boeing-747

Jianzhuang Huang and N. Eva Wu
Department of Electrical Engineering, Binghamton University, Binghamton, NY 13902-6000
jhuang5, evawu@binghamton.edu

Abstract—**In this paper, real time monitoring of the control system of a Boeing 747 aircraft (B747) is considered by using a pulse-compression probing method. The method extracts small signal characteristics of the targeted system, and detects deviations from the system's normal behavior with high sensitivity. This paper demonstrates, through a simulated model of a B747 longitudinal motion, the successful application of the probing method in monitoring a nonlinear dynamic system. The paper focuses on the process of determining suitable probing signals and probing structure for the B747, and discusses the monitoring results for two major types of faults in its actuators.**

I. Introduction

RESEACH is being conducted at NASA on assessment of reliable flight envelope for B747 based on real time information [8]. An important part of the research is focused on real-time prognosis and monitoring of the system. The pulse-compression probing method, first introduced in 1995 [1], is applied to a nonlinear longitudinal model of the B474-100/200 aircraft in this work for proof of concept of prognosis with small signal probing [3]. This method uses a similar principle to that used in the cross-correlation technique described in [6] with a vastly different implementation. The first application of the pulse compression method to monitoring a dynamic system was reported in 2001 [9], where a linear hydraulic system model was the subject of study.

From the system identification point of view, the pulse-compression method extracts the small signal characteristics of a system by compressing a small and long probing input into an equivalent impulse-like narrow wavelet, which then effectively excites the system and produces a probing output that resembles the impulse response of the system. From the system monitoring point of view, deviation of the probing output from the normal impulse response of the system indicates a change in the system. It is possible to identify faults by analyzing the probing output

New challenges in monitoring the B747 lie with the nonlinearity of the system, and with its multiple inputs and multiple outputs, as well as the closed-loop structure. The nonlinearity is dealt with in this paper by recognizing that the pulse-compression method uses small but elongated probing signal to create the effect of an impulse, and therefore is applicable to monitoring those nonlinear systems whose major faults can be captured in small signal probing responses. These include the common actuator-surface faults.

The parameters of the probing signal determine how closely the probing output resembles the impulse response of the linearized B747 dynamic model around a trim point when there is no fault, how much effect the probing signal has on the system's normal behavior, and how much memory and computation are required to achieve a probing of a sufficient resolution. As a result, probing signal design is one of the most important steps for monitoring systems using pulse-compression method.

The paper is organized as follows. Section II reviews the pulse-compression probing method developed for linear system. Section III applies the method to a nonlinear model of the longitudinal motion of a B747. Section IV presents and analyzes some results of monitoring on B747. Section V concludes the paper.

II. Review of Pulse-Compression Probing Method For Linear Systems

The principle of the pulse compression method is reviewed in this section. The presentation draws heavily from [9]. Its applicability to nonlinear system is discussed in the next section through a B747 monitoring example.

For a linear system modeled by its impulse response *h(t)* with an input *u(t)*, the system output is $y(t) = h(t) * u(t)$, where '*' denotes the convolution operation. One way to monitor the system is to inject a probing signal $\rho(t)$ at the system input, and process the system output to generate a probing output

$$z(t) = y(t) \otimes s(t) = h(t) * \rho(t) \otimes s(t), \quad (1)$$

where '$\otimes$' denotes the correlation operation and *s(t)* is a reference signal. Let *e(t)* represents the equivalent operation of $\rho(t) \otimes s(t)$, then

$$z(t) = h(t - T) * e(t), \quad (2)$$

where *T* is a time delay due to the correlation operation. The presence of *T* is suppressed until we are ready to elaborate on it. By carefully selecting $\rho(t)$ and *s(t)* that make *e(t)* close to the delta function $\delta(t)$, the probing output *z(t)* can approach the impulse response *h(t)* of the system. System

This work was supported in part by the NASA under Grant NNX08AC65A.

monitoring amounts to identifying the deviation of *z(t)* from *h(t)*.

Additional challenge arises when monitoring a system while it is in operation. In this case, the system output is the combination of the measured system output $y_1(t)$ and an extra output $y_2(t)$ due to probing, i.e.,

$$\begin{aligned} y(t) &= y_1(t) + y_2(t) \\ &= h(t) * u(t) + h(t) * \rho(t) . \end{aligned} \tag{3}$$

The probing output of the system becomes

$$z(t) = z_1(t) + z_2(t) ,$$

where

$$z_1(t) = y_1(t) \otimes s(t) = h(t) * u(t) \otimes s(t) \tag{4}$$

$$\begin{aligned} z_2(t) &= y_2(t) \otimes s(t) = h(t) * \rho(t) \otimes s(t) \\ &= h(t) * e(t) . \end{aligned} \tag{5}$$

In view of the system operation, $y_2(t)$ is an undesired output that disturbs the normal system output $y_1(t)$, and thus considered as noise at the system output. In view of system monitoring, $z_1(t)$ is an undesired component in the probing output, and this considered as noise. As a result, two goals need to be accomplished simultaneously by designing the probing signal $\rho(t)$ and the reference signal *s(t)*. The first goal is to minimize the noise $y_2(t)$ in the system output so that *y(t)* is approximately equal to $y_1(t)$. The second goal is to minimize the noise $z_1(t)$ in the probing output so that *z(t)* is approximately equal to $z_2(t)$.

The proposed design for *s(t)* and $\rho(t)$ in [1], allows to achieve both goals: *s(t)* is selected to be an impulsive single period pseudo-random binary sequence (*PRBS*) with order *n* and bit duration t_0, and $\rho(t)$ is selected to be a cyclic repetition of $\eta(t) * s(t)$, where $\eta(t)$ is a narrow low pass rectangular wavelet with unity amplitude and pulse width t_0. The period *T* of $\rho(t)$ is equal to $(2^n - 1) * t_0$. The amplitude of $\rho(t)$ and *s(t)* might be different. Let *a* represent the amplitude of $\rho(t)$, and *b* represent the amplitude of *s(t)*. Figure 1 shows an example of *s(t)* and $\rho(t)$ for *a*=*b* and *n*=5.

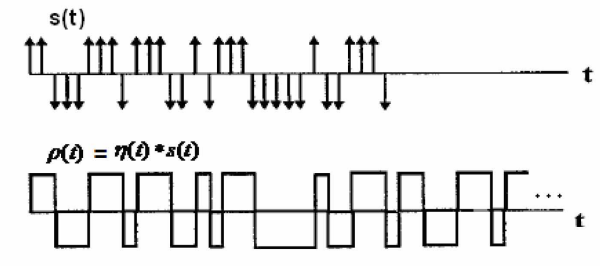

Fig. 1. Example of reference signal *s(t)* and probing signal $\rho(t)$.

Let $PRBS_{norm}$ represent the normalized *PRBS* shifting between ± 1. According to [5] and [7], discrete *PRBS* with order *n* and amplitude *a* has the following two properties:

$$\begin{aligned} &\left| \frac{1}{2^n - 1} \sum_{k=1}^{2^n - 1} PRBS(k) \right| \\ &= \left| \frac{a}{2^n - 1} \sum_{k=1}^{2^n - 1} PRBS_{norm}(k) \right| = \frac{a}{2^n - 1} ; \end{aligned} \tag{6}$$

$$\begin{aligned} &\frac{1}{2^n - 1} \sum_{k=1}^{2^n - 1} PRBS(k) \cdot PRBS(k + l) \\ &= \frac{a^2}{2^n - 1} \sum_{k=1}^{2^n - 1} PRBS_{norm}(k) \cdot PRBS_{norm}(k + l) \\ &= \begin{cases} a^2, & l = 0, \pm(2^n - 1), \pm 2(2^n - 1), ... \\ -\dfrac{a^2}{2^n - 1}, & elsewhere \end{cases} \\ &= \frac{a^2}{2^n - 1} \cdot \{ 2^n \cdot [\sum_k \delta_d (l - k \cdot (2^n - 1))] - 1 \} , \end{aligned} \tag{7}$$

where $\delta_d(l)$ is the discrete pulse with unity amplitude. (7) holds only if one of the *PRBS(k)* is cyclically repeated. Applying (7) to *e(t)*,

$$\begin{aligned} e(t) &= \rho(t) \otimes s(t) \\ &= \eta(t) * \frac{a \cdot b}{T} \cdot \sum_i \sum_{k=1}^{2^n - 1} PRBS_{norm}(k) \cdot PRBS_{norm}(k + it_0) \\ &= \frac{a \cdot b}{T} \cdot \{ 2^n \cdot [\eta(t) * \sum_k \delta(t - k \cdot (2^n - 1) \cdot t_0)] - 1 \} \\ &= \frac{a \cdot b}{t_0} \cdot \frac{2^n \cdot [\eta(t) * \sum_k \delta(t - kT)] - 1}{(2^n - 1)} . \end{aligned}$$

With sufficiently large *n*,

$$\begin{aligned} e(t) &\approx \frac{a \cdot b}{t_0} \cdot \eta(t) * \sum_k \delta(t - kT) \\ &= \frac{a \cdot b}{t_0} \cdot \sum_k \eta(t - kT) . \end{aligned} \tag{8}$$

By substituting (8) into (5),

$$\begin{aligned} z_2(t) &= h(t) * e(t) \\ &\approx h(t) * \frac{a \cdot b}{t_0} \cdot \sum_k \eta(t - kT) . \end{aligned} \tag{9}$$

Since $\eta(t)$ is a rectangular wavelet with pulse width of t_0, with sufficiently small t_0,

$$\frac{1}{t_0}\cdot\eta(t)\approx\delta(t)\,. \tag{10}$$

As a result,

$$z_2(t)\approx h(t)*a\cdot b\sum_k\delta(t-kT)\approx a\cdot b\sum_k h(t-kT)\,. \tag{11}$$

In order for $z_2(t)$ to resemble the impulse response,

$$a\cdot b=1\,. \tag{12}$$

When $z_2(t)$ dominates $z(t)$, the probing output is a cyclic repetition of the impulse response $h(t)$ with a period of T. However, noise will be introduced to the first period due to the correlation operation. The actual repetition starts after a time delay of T. Therefore, T should always be minimized to reduce the time for getting the probing output. In order to avoid time domain aliasing, T has to be longer than the time for $h(t)$ to be settled down to zero. As a result, the optimal selection of T should be the time as soon as $h(t)$ settles down to zero. Recall that

$$T=(2^n-1)\cdot t_0\,. \tag{13}$$

When T is fixed, n would be disproportional to t_0. t_0 is the bit duration of the impulsive *PRBS*, and the pulse width of $\eta(t)$. It could be interpreted as the sampling time of $h(t)$, and determines the level of details of $h(t)$ to be extracted in the probing output. As a result, t_0 has to satisfy the sampling theorem described in [4] and [10]. With occurrences of signal attenuation, a practical choice for the sampling frequency f_s would be at least 5 times of the system bandwidth ω_{BW}. As a result,

$$t_0=\frac{1}{f_s}\le\frac{2\pi}{5\omega_{BW}}\,. \tag{14}$$

Solving n from (13),

$$n=\log_2\left(\frac{T}{t_0}+1\right)\ge\log_2\left(\frac{5\omega_{BW}T}{2\pi}+1\right)\,. \tag{15}$$

The signal to noise ratio (*SNR*) of the system output is

$$SNR_s=\frac{rms\{y_1(t)\}}{rms\{y_2(t)\}}=\frac{rms\{h(t)*u(t)\}}{rms\{h(t)*\rho(t)\}}\,. \tag{16}$$

In order to increase SNR_s, the amplitude a of $\rho(t)$ should be decreased. Because of (12), the amplitude b of $s(t)$ should be increased to eliminate the change in $z_2(t)$. Since $z_1(t)$ is the correlation output between $y_1(t)$ and $s(t)$, the magnitude of $z_1(t)$ would also be increased, causing the *SNR* of the probing output to decrease:

$$SNR_z=\frac{rms\{z_2(t)\}}{rms\{z_1(t)\}}\,. \tag{17}$$

Amplitude a of the probing input signal affects the system output in the opposite way as it affects the probing output. It has to be selected carefully to give optimal *SNR* for both the system output and the probing output.

III. Pulse-Compression Probing for B747

The pulse-compression probing method has been successfully applied to monitoring single-input and single-output linear systems [9]. This section establishes its applicability to a multivariable nonlinear system with one basic goal in mind: to reveal the smallest possible change from normal probing output as soon as a fault occurs that causes the change. The quantification on how small and how soon will be reported in the future through statistical analysis of the probing output.

Although the derivations in the previous section were based on linear systems, we argue that small signal behaviors of nonlinear systems are very similar to that of linear systems using the B747 model [2], [3] as a test-bed to support our theory. Consider an incremental model of the general plant describing the aircraft operation around some trim point (x_{trim},u_{trim})

$$\begin{aligned}&\dot{x}_{trim}(t)=f(x_{trim},u_{trim})=0\\&\dot{\tilde{x}}=\underbrace{\left.\frac{\partial f}{\partial x}\right|_{(x_{trim},u_{trim})}}_{A(x_{trim},u_{trim})}\tilde{x}+\underbrace{\left.\frac{\partial f}{\partial u}\right|_{(x_{trim},u_{trim})}}_{B(x_{trim},u_{trim})}\tilde{u}\\&y=x_{trim}+\tilde{x}\,.\end{aligned} \tag{18}$$

The multivariable small signal impulse response for a normal system to be involved at a given trim point is

$$H(t)=\mathcal{L}^{-1}[sI-A(x_{trim},u_{trim})]^{-1}B(x_{trim},u_{trim})\,. \tag{19}$$

This view of small signal analysis extends to a closed-loop model with a linear controller to which a small external signal is injected at the plant input and response measured at the plant output. In this case, the controller states also enter the first and second equations above. When sampled, (19) gives the sequence of Markov parameters of a system that are to be captured in the probing output without the knowledge of other parameters about the system.

Figure 2 contains a block diagram of a model of B747. This model is the nonlinear longitudinal motion model of B747 series 100/200 as described in [2] and [3]. In [2], complete nonlinear equations of longitudinal motion of the aircraft together with the aerodynamic forces, moments and coefficients are presented in detail. In [3], an accompanying software package of a 2003 version of Flight Lab 747 is provided with the nonlinear B747 model implemented in Simulink environment.

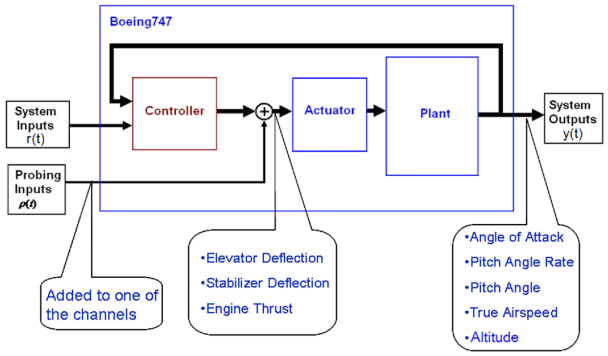

Fig. 2. Block diagram of B747 model.

In this paper, faults used to test the probing method are confined to those associated with actuators for stabilizers and for elevators, and with the engines to a lesser degree. These faults are being parameterized in a parallel effort to estimate their severity using a modified version of the two-stage Kalman filter approach initially developed in [8]. In this parallel effort the probing signal also serves to provide the excitation necessary for the estimation of the parameters.

To better capture the actuator faults, a probing signal $\rho(t)$ is injected to the input of one of the elevator deflection (*de*), stabilizer deflection (*ds*) and the engine thrust (*et*) channels. There are five outputs in the system: angle of attack (*alpha*), pitch angle rate (*q*), pitch angle (*theta*), true airspeed (*V*) and altitude (*h*).

Since the probing signal parameter selection depends on the specific input and output, the following analysis focuses on the response of alpha to de at the trim point

$$x_{trim} = [0.0162(rad);\ 0(rad/sec);\ 230(m/sec);\ 0.0162(rad);\ 7000(m)]$$
$$u_{trim} = [0(rad);\ 0.00128\ (rad);\ 41631(N)] \quad (20)$$

Similar analyses can be applied to the remaining 14 input-output channels.

The values of four parameters, period T, bit duration t_0, order n, and amplitude a, in the probing signal are now considered. Recall that the optimal selection of T is the settling time for the impulse response when time to detect a change is constrained. This time can be determined using the impulse response describing linearized B747 model at trim point (20) from *de* to *alpha*, which is shown in Figure 3. The figure indicates that the impulse response is settled down to zero between 8 to 10 seconds. To minimize time domain aliasing, T is set to 10 seconds.

According to (14) in the previous section, the upper limit of t_0 depends on the bandwidth of the system. The bandwidth is determined from the frequency response of the same linearized model to be about 9 Hz, or

$$\omega_{BW} = 9 \cdot 2\pi \ \ rad/sec.$$

Substitute ω_{BW} into (15),

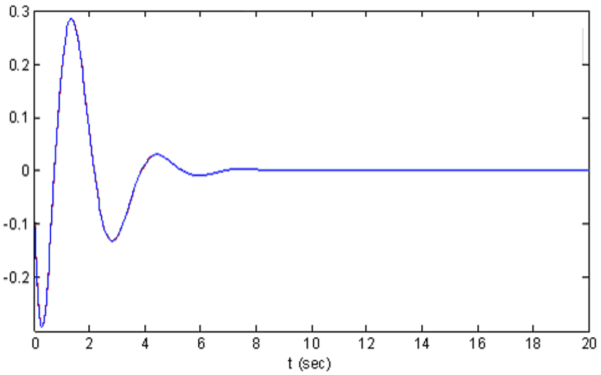

Fig. 3. Impulse response of the linearized model.

$$n \ge \log_2\left(\frac{5\omega_{BW}T}{2\pi}+1\right) \ge \log_2\left(\frac{5\cdot 9\cdot 2\pi\cdot 10}{2\pi}+1\right) \approx 8.8 \cdot$$

Therefore, the order of the probing signal has to be at least 9. The bit duration t_0 becomes

$$t_0 = \frac{T}{(2^n-1)} = \frac{10}{(2^9-1)} \approx 19.6ms \cdot$$

The last parameter that needs to be determined is the amplitude a of the probing signal. As described in the previous section, a has different effects on the system output and on the probing output. Figure 4 shows the system outputs and probing outputs as well as their *SNR*s when the amplitude of the probing signal is increased from 0.1 to 10.

Figure 4 indicates that the minimum 20dB *SNR*s proposed cannot be satisfied simultaneously at both outputs. In order to improve the *SNR*s, the technique of system output cancelation is applied. Figure 5 shows such a schematic. Depending on how the duplicated model is constructed and how close it is to the system, the difference between $y_1(t)$ and $y_1'(t)$ can be as low as zero. If they are perfectly matched, $y_1(t)$ would be totally eliminated before the correlation operation. As a result, the noise in the probing output will be minimized, and the effect of A on the probing output will also be minimized. However, if $y_1'(t)$ deviates a

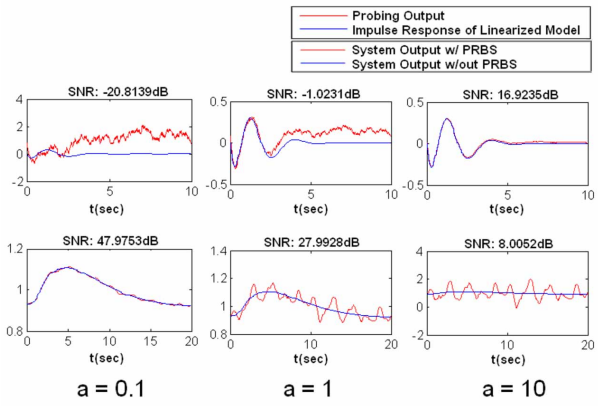

Fig. 4. Effects of probing input amplitude a on both system output and probing output.

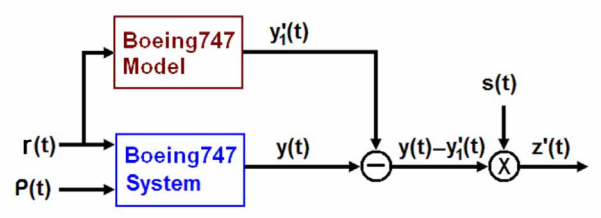

Fig. 5. Block diagram of system output cancelation technique.

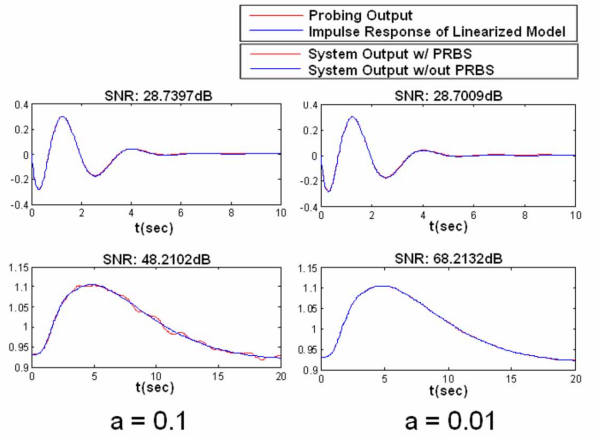

Fig. 6. Effects of amplitude a with output cancelation.

lot from $y_1(t)$, extra noise will be introduced in the probing output, and that would cause trouble in resembling the impulse response. This thesis will assume that the duplicated system matches the system well. Figure 6 shows the noticeable improvement in *SNR*s after applying the cancelation technique. Probing signal amplitude a = 0.01 is selected for monitoring the B747.

To summarize, the values of the four parameters of the probing signal used at elevator deflection channel for monitoring the nonlinear B747 system operating at trim point (20) are set at: T = 10 seconds (probing delay or sequence period), n = 9 (probing sequence order), t_0 = 19.6 ms (probing sequence bit duration), a = 0.01 (amplitude of probing signal).

IV. Results of Monitoring

In principle, the pulse compression probing should detect changes due to any faults that alter the small signal impulse response in a channel. This section selects, as test cases, stuck and loss of effectiveness faults in the elevator deflection channel of the B747. To model a stuck fault in the i^{th} channel, the i^{th} control input is replaced by constant value; and to model the loss of effectiveness in the i^{th} channel, a factor valued between 0 and 1 is attached to the i^{th} control input.

Stuck faults ranging from -23° to 17° are injected in the elevator deflection channel. The angle of attack is processed to obtain the probing output, as shown in Figure 7 for different levels of actuator stuck. Signal to noise at the probing output is calculated by

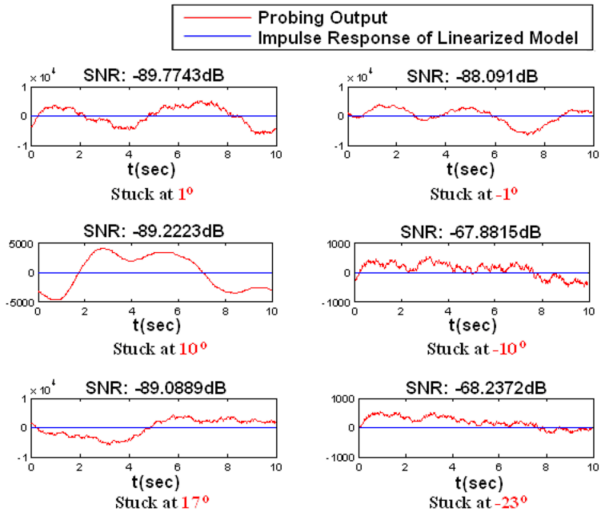

Fig. 7. Stuck fault in the elevator deflation channel.

$$SNR_z = \frac{rms\{h(t)\}}{rms\{z(t) - h(t)\}}. \qquad (21)$$

(17) and (21) are almost identical when there is no fault, in which case $z_2(t) \cong h(t)$. By using (21), the signal always stays the same, but the noise increases when faults occur.

Comparing the *SNR* of the probing output shown in Figure 7 to the *SNR* of the probing output in the normal case shown in Figure 6, the difference is obvious. The stuck fault in elevator deflection channel can be easily identified by monitoring the *SNR* of the probing output.

Stuck faults ranging from -12° and 3° in the stabilizer channel have also been experimented, and similar conclusions to those in the elevator stuck fault experiments are drawn.

Without an extensive analysis of the waveforms of the probing outputs, or a careful construction of the probing structure, however, one is not able to easily distinguish stuck faults of different channels. These solutions have been actively pursued currently. For now, we are content with the high sensitivity of the probing outputs to the occurrence of the stuck faults.

Figure 8 shows the change in the probing output when a range of loss of effectiveness occurs in elevator deflection channel. It is seen that a higher percentage loss produces lower *SNR* in the probing output. Therefore, as long as the threshold *SNR* for loss of effectiveness fault is set, the faults of different levels can be identified by comparing the actual *SNR* to the threshold *SNR*. The figures also indicate that the *SNR* values for loss of effectiveness fault are much higher than those for stuck faults, which can be useful to distinguish the two types of faults. Again the source of a fault can not be isolated without a careful analysis of the probing outputs, and a careful construction of probing structure.

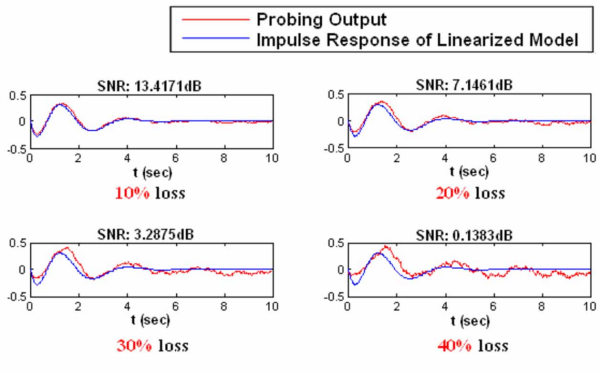

Fig. 8. Loss of effectiveness fault in the elevator deflation channel.

V. CONCLUSION

In this paper, a small signal probing concept using the pulse-compression method is shown to be effective in revealing changes in nonlinear systems. Probing signals are designed for the model of longitudinal motion of a Boeing 747 aircraft. The probing outputs are sensitive to stuck faults, responsive to loss of effectiveness in actuators. Ongoing investigations include analysis of probing output, development of fault isolation logic, and implementation of the probing algorithms using field-programmable gate array (*FPGA*).

REFERENCES

[1] Chen, H., and Wu, N. E., *A method of high resolution and high SNR data acquisition for probing using pulse-compression*, US Pat. 5,426,618, 1995.

[2] Esteban, A.M., *A linear Parameter Varying Model of the Boeing 747-100/200: Longitudinal Motion*, MS Thesis. University of Minnesota, 2001.

[3] Esteban, A.M. and Balas, G.J, *A Boeing 747-100/200 Aircraft Fault-Tolerant and Fault Diagnostic Benchmark*, Technical Report AME-UoM-2003-1, University of Minnesota, 2003.

[4] Gene F. Franklin, J. David Powell, *Digital Control of Dynamic Systems*, Addison-Wesley Publishing Company, pp.276, 1980.

[5] Golomb, S.W., *Digital Communication with Space Applications,* Prentice Hall, 1964. *Shift Register Sequences,* Holden-Day, 1976.

[6] Hill, J.D., and McMurtry, G.J., "An Application of Digital Computers to Linear System Identification", *IEEE Trans. on Automatic Control*, vol. 19, pp.753-768, 1974.

[7] Ljung, L., *System Identification: the Theory for the User,* Prentice-Hall, 1999.

[8] Shin, J-Y., Wu, N.E., and Zhang. Y., "Dynamic Flight Envelope Assessment and Prediction", *NASA Aviation Safety-Integrated Resilient Aircraft Control (IRAC)*, Subtopic IRAC1-3, NASA, 2007.

[9] Wu, N.E., and Wang X., "A Pulse Compression Method for Process Monitoring", *American Control Conference*, Arlington, VA, pp.2127-2132, 2001.

[10] Zieme, R.E., Peterson, R.W., *Introduction to Digital Communication*, Prentice Hall, 2000.